

Strongly gapped spin-wave excitation in the insulating phase of NaOsO₃S. Calder,^{1,*} J. G. Vale,^{2,3,†} N. Bogdanov,⁴ C. Donnerer,² D. Pincini,^{2,5} M. Moretti Sala,⁶ X. Liu,^{7,8} M. H. Upton,⁹ D. Casa,⁹ Y. G. Shi,^{8,10} Y. Tsumimoto,¹⁰ K. Yamaura,^{10,11} J. P. Hill,⁷ J. van den Brink,⁴ D. F. McMorrow,² and A. D. Christianson^{1,12}¹*Quantum Condensed Matter Division, Oak Ridge National Laboratory, Oak Ridge, Tennessee 37831, USA*²*London Centre for Nanotechnology and Department of Physics and Astronomy, University College London, Gower Street, London WC1E 6BT, United Kingdom*³*Laboratory for Quantum Magnetism, Ecole Polytechnique Fédérale de Lausanne (EPFL), CH-1015 Lausanne, Switzerland*⁴*Institute for Theoretical Solid State Physics, IFW Dresden, D-01171 Dresden, Germany*⁵*Diamond Light Source Ltd, Diamond House, Harwell Science and Innovation Campus, Didcot, Oxfordshire OX11 0DE, United Kingdom*⁶*European Synchrotron Radiation Facility, BP 220, F-38043 Grenoble Cedex, France*⁷*Condensed Matter Physics and Materials Science Department and National Synchrotron Light Source-II, Brookhaven National Laboratory, Upton New York 11973, USA*⁸*Beijing National Laboratory for Condensed Matter Physics and Institute of Physics, Chinese Academy of Sciences, Beijing 100190, China*⁹*Advanced Photon Source, Argonne National Laboratory, Argonne, Illinois 60439, USA*¹⁰*Research Center for Functional Materials, National Institute for Materials Science, 1-1 Namiki, Tsukuba, Ibaraki 305-0044, Japan*¹¹*Graduate School of Chemical Sciences and Engineering, Hokkaido University, North 10 West 8, Kita-ku, Sapporo, Hokkaido 060-0810, Japan*¹²*Department of Physics and Astronomy, University of Tennessee, Knoxville, Tennessee 37996, USA*

(Received 23 August 2016; revised manuscript received 7 December 2016; published 23 January 2017)

NaOsO₃ hosts a rare manifestation of a metal-insulator transition driven by magnetic correlations, placing the magnetic exchange interactions in a central role. We use resonant inelastic x-ray scattering to directly probe these magnetic exchange interactions. A dispersive and strongly gapped (58 meV) excitation is observed, indicating appreciable spin-orbit coupling in this 5*d*³ system. The excitation is well described within a minimal model Hamiltonian with strong anisotropy and Heisenberg exchange ($J_1 = J_2 = 13.9$ meV). The observed behavior places NaOsO₃ on the boundary between localized and itinerant magnetism.

DOI: [10.1103/PhysRevB.95.020413](https://doi.org/10.1103/PhysRevB.95.020413)

The underlying mechanisms driving a metal-insulator transition (MIT) are an enduring focus of condensed matter physics [1]. Recent interest has extended investigations to 5*d*-based transition metal oxides that host new paradigms of competing interactions, creating novel MITs [2]. For example, spin-orbit coupling (SOC) in 5*d*⁵ iridates dramatically influences the electronic ground state to allow even the presence of the reduced on-site Coulomb interaction (U) to drive a relativistic Mott MIT [3]. Conversely, in 5*d*³ osmium-based compounds, MITs occur that cannot be reconciled with the reduced U in 5*d* systems, even when the large SOC is taken into account. These compounds therefore fall outside the Mott approximation. Of particular interest in this regard are the osmates NaOsO₃ and Cd₂Os₂O₇, which undergo a MIT that is continuous and coincident with the onset of magnetic order, indicating the central role of magnetic interactions in the transition [4–7]. Accessing the collective role of the competing inter-ion and intra-ion electron-electron interactions, SOC, and magnetism in driving the MIT is required to gain an understanding of the novel MITs in these osmates.

Outside of a Mott MIT, several other mechanisms exist to describe a MIT, including an Anderson MIT driven by disorder [8] and a Peierls MIT driven by a structural distortion in a low-dimensional system [9]. Slater considered a route in which magnetism could drive a MIT, with the central observation being that within a magnetically ordered system,

the potential created by an up spin is different from that created by a down spin [10]. By this definition, three-dimensional magnetic ordering with oppositely aligned spins is a route to a MIT, and implicitly includes $q = 0$ antiferromagnetic structures. NaOsO₃ exhibits several features consistent with Slater's general scenario [6,7,11–15]. The MIT occurs concomitant with the onset of antiferromagnetic ordering ($T_N = T_{MIT} = 410$ K) that can create a periodic potential. Furthermore, in NaOsO₃, the MIT is continuous and no structural symmetry change occurs. However, several important questions have so far remained experimentally inaccessible, hindering the development of further insight into the mechanism of this unusual MIT and prohibiting a quantitative description beyond the mean-field approach invoked by Slater for a magnetic MIT.

Principally, since the MIT is driven by magnetic ordering, the magnetic exchange interactions (J) are central to the creation of the MIT in NaOsO₃. Therefore, measuring the dominant exchange pathways and interactions is required to build robust models of the MIT. Additionally, the energy scales of the interactions that are required to describe the electronic behavior, such as crystal field splitting, Hund's coupling, and SOC, have not been accessed. In particular, the nominal 5*d*³ electronic occupancy suggests zero orbital angular momentum in the L - S coupling limit, and previous experimental descriptions did not require the inclusion of strong SOC. However, mounting experimental evidence in other 5*d*³ systems indicates SOC is required to describe the magnetism [16–18]. To answer these questions, we performed resonant inelastic x-ray scattering (RIXS) to directly probe the 5*d* electrons of the Os ion in NaOsO₃.

*caldersa@ornl.gov

†j.vale@ucl.ac.uk

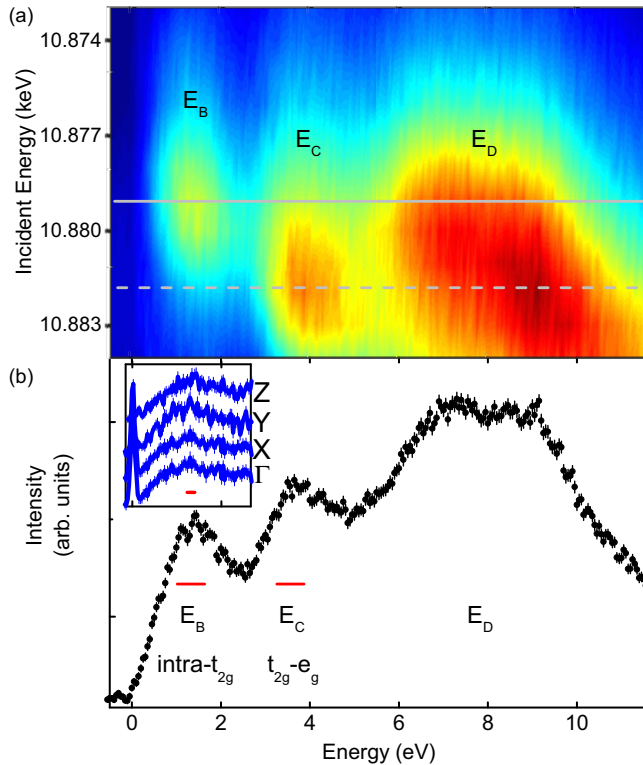


FIG. 1. (a) Excitations measured in NaOsO₃ at various fixed incident energies through the Os *L* edge using RIXS. Three inelastic peaks are observed, labeled E_B , E_C , and E_D . The solid (dashed) gray line indicates the incident energy that yields the maximum intensity for E_B (E_C). (b) RIXS measurement at a fixed incident energy of 10.88 keV. The main panel was measured with a resolution of $\Delta E = 275$ meV and the inset data were collected with $\Delta E = 46$ meV. The horizontal red lines indicate the full width at half maximum (FWHM) experimental resolution. Measurements were performed at 300 K.

RIXS measurements at the Os *L*₃ edge (10.87 keV) were performed on the ID20 spectrometer at the ESRF, Grenoble. A single crystal of NaOsO₃, space group *Pnma*, was oriented with the (*HOL*) plane normal to the sample surface. The scattering plane and incident photon polarization were both horizontal. The incident beam was focused to a size of $20 \times 10 \mu\text{m}^2$ (*H* × *V*) at the sample position. Measurements were performed with low- ($\Delta E = 275$ meV) and high-resolution ($\Delta E = 46$ meV) setups by switching between a Si(311) channel-cut secondary monochromator and a (664) four-bounce, respectively. Both setups used a Si(664) diced spherical analyzer at 2 m radius from the detector. Preliminary measurements were performed at the Advanced Photon Source (APS) on the MERIX instrument using an identical setup to that described in Ref. [18].

We begin by considering the results using the low-resolution setup ($\Delta E = 275$ meV) before focusing on our main finding of a spin-wave excitation with high-resolution measurements ($\Delta E = 46$ meV). A RIXS map of the orbital excitations, that involve intra or inter *d-d* transitions, in NaOsO₃ obtained by measuring the inelastic energy loss spectrum at several fixed incident energies through the Os *L*₃ resonant edge, is shown in Fig. 1(a) at 300 K. Three

broad inelastic features are observed, labeled E_B , E_C , and E_D . On a qualitative level the excitations appear analogous to RIXS measurements on $5d^3$ -based Cd₂Os₂O₇ [18] and exhibit notable differences from measurements of $5d^5$ -based iridates [19]. The incident energy dependence of features E_B and E_C in the RIXS map is consistent with a nominal splitting of the $5d$ manifold into states with t_{2g} and e_g symmetry, with the scattering following dipole selection rules ($\Delta S = 1$). E_B involves intra- t_{2g} transitions whereas E_C is due to t_{2g} - e_g excitations. We assign excitation E_D to ligand-metal charge transfer (LMCT).

The inelastic excitation E_B is centered at 1.27(2) eV and corresponds to intra- t_{2g} transitions. As shown in the inset of Fig. 1(b), even when measured with the high-resolution RIXS setup, E_B remained as a broad single-peaked excitation, significantly broader than the instrumental resolution of 46 meV. This makes any splitting of the t_{2g} manifold from SOC or a structural distortion unresolvable in NaOsO₃. This contrasts to the case of the iridium-based relativistic Mott insulators, where SOC strongly splits the t_{2g} electronic ground state into $J_{\text{eff}} = \frac{1}{2}$ and $J_{\text{eff}} = \frac{3}{2}$ bands and results in a measured splitting of E_B [19,20]. Since E_B consists of intra- t_{2g} transitions, we follow the reasoning outlined in Ref. [18] to experimentally define the Hund's coupling energy (J_H) value in NaOsO₃ as $J_H = 1.27 \text{ eV}/3.75 = 0.34 \text{ eV}$ based on the center of E_B . The 3.75 factor derives from the consideration of E_B as consisting of eight $S = \frac{1}{2}$ states, five of which have relative energy $3J_H$ and three having $5J_H$, yielding an average of $3.75J_H$. We note that since any underlying splitting of E_B is unresolved, this is an approximate measurement of J_H , and, however, is useful for comparing with similar $5d^3$ systems such as Cd₂Os₂O₇.

Excitation E_C is located at 3.6(1) eV and is a direct measure of the crystal field splitting. NaOsO₃ and Cd₂Os₂O₇ have a similar local OsO₆ octahedral environment, however, the t_{2g} - e_g splitting is 0.9 eV lower in NaOsO₃ [18]. This indicates that considerations beyond the local $5d$ octahedral environment are crucial, which is in line with expectations of the importance of the spatially extended $5d$ orbitals.

The magnetic order and consequently the magnetic exchange interactions are central to the creation of the MIT in NaOsO₃. Therefore, measuring and modeling the dominant exchange pathways is required to yield a complete picture of the MIT. The crystal size of NaOsO₃ is currently beyond the limits of inelastic neutron scattering, however, RIXS offers a route to quantitatively probe the collective magnetic excitations in $5d$ systems [19]. The low-energy scattering for NaOsO₃ using high-resolution Os RIXS is shown in Fig. 2. Measurements along high-symmetry directions shows a single resolution limited inelastic excitation (E_A). The excitation, along with the elastic line, were fit with a Gaussian peak shape to follow the dispersion. Figure 3(a) reveals E_A is strongly dispersive, indicative of a spin-wave excitation. The bandwidth is ~ 80 meV with maxima at the zone boundary along the *Z* and *X* directions and a reduced energy at *Y*. A large spin gap of 58 meV is observed at the zone center (Γ) that signifies the presence of strong anisotropy in NaOsO₃.

To provide a quantitative description of the magnetic excitations, we invoke a minimal model Hamiltonian with

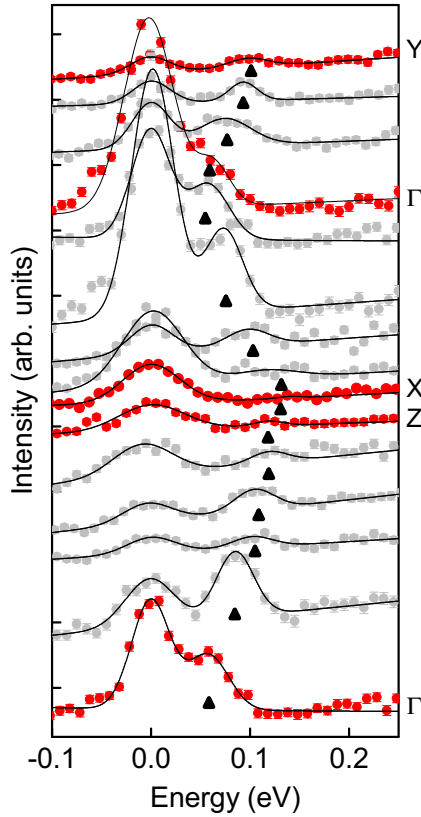


FIG. 2. RIXS measurements of NaOsO₃ at 300 K along high-symmetry directions in the Brillouin zone. The line shows the fit to the elastic and inelastic scattering at E_A , with the position of E_A indicated by the triangles. The data have been offset to aid comparison. The strong variation of the elastic line intensity is due to moving through the ideal $2\theta = 90^\circ$ RIXS condition where elastic scattering is suppressed.

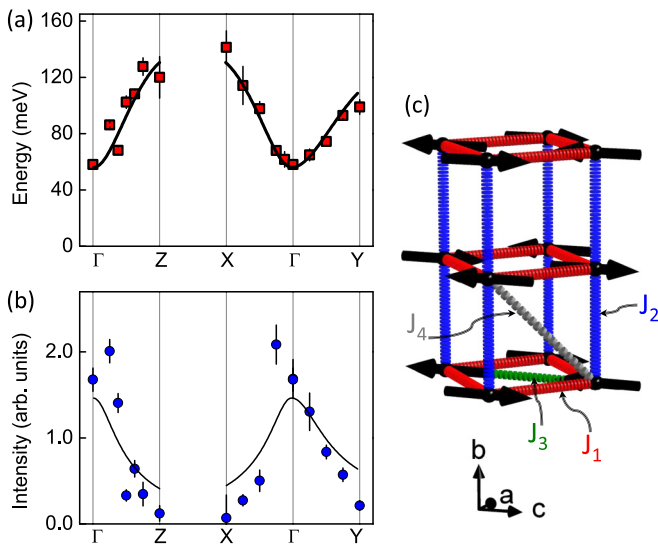


FIG. 3. (a) Measured (squares) and calculated (line) dispersion of E_A along high-symmetry directions. (b) Measured (circles) and calculated (line) intensity of E_A . (c) The calculations were performed using Eq. (1), a minimal model Hamiltonian with the exchange interactions $J_1 = J_2 = 13.9$ meV.

nearest-neighbor (nn) and next-nearest-neighbor (nnn) exchange interactions:

$$\mathcal{H} = J_1 \sum_{nn} \mathbf{S}_i \cdot \mathbf{S}_j + J_2 \sum_{nnn} \mathbf{S}_i \cdot \mathbf{S}_j + \Delta. \quad (1)$$

A SOC induced anisotropic term is included to account for the gap. For the case of symmetric exchange anisotropy, $\Delta = \Gamma \sum_{nn,nnn} S_i^z S_j^z$, and for single-ion anisotropy, $\Delta = D \sum (S_i^z)^2$.

The RIXS data for NaOsO₃ were modeled within a linear spin-wave (LSW) approximation [21] and the results checked against numerical calculations using SpinW [22]. The nominal spin-only value of $S = \frac{3}{2}$ was used throughout. Fitting the experimental dispersion to Eq. (1) produces close agreement to both the dispersion and corresponding intensity (Fig. 3), indicating the minimal model Hamiltonian captures the essential features and consequently provides an experimental assignment of the dominant magnetic exchange interactions and their energy. The fitting yields $J_1 = J_2 = 13.9(5)$ meV and $\Gamma = 1.4(1)$ meV. Allowing J_1 and J_2 to vary independently did not improve the fit, reflecting the pseudocubic nature of the structure. Adding a third-nearest-neighbor term J_3 , or $J_3 = J_4$, to recover the cubic limit, alters the energy at Z with respect to X, however, within resolution the measured energy at $X = Z$. Therefore, we conclude that exchange interactions J_3 and above have a magnitude appreciably less than J_1 or J_2 and limit the Hamiltonian to Eq. (1). Consequently, NaOsO₃ is well described by dominant nearest-neighbor magnetic interactions in three dimensions forming a robust G -type antiferromagnetic order in this perovskite. Replacing exchange anisotropy with a single-ion anisotropy [$D \sum (S_i^z)^2$] term yields the same J_1 and J_2 values and $D = 4$ meV.

The mechanism for the spin gap is effectively disconnected from the magnetic exchange interactions in Eq. (1). However, the presence of such a large spin gap is significant in terms of the underlying physics in NaOsO₃. In particular, all possible mechanisms to open a spin gap, single-ion anisotropy (SIA), the Dzyaloshinskii-Moriya (DM) interaction, and exchange anisotropy, require SOC. We briefly consider how the anisotropies influence NaOsO₃. SIA arises due to a noncubic environment and in NaOsO₃ the OsO₆ octahedra are weakly trigonally and tetragonally compressed. However, such a large gap due to SIA does not appear consistent with the reduced spin gaps of 15–20 meV observed in other $5d^3$ osmates with similar distortions [17]. In NaOsO₃ a nonzero local DM vector exists since the oxygen mediating the superexchange interaction between the two Os sites does not sit at an inversion center. Experimentally, there is evidence of weak ferromagnetism [6], however, the spin canting producing this was undetectable with neutron diffraction [7]. This would suggest that the DM interaction, while present, is weak to first order. Exchange anisotropy, a pseudodipolar effect, results as a consequence of second-order SOC effects between neighboring Os ions, and hence is generally weaker than the DM interaction and SIA. However, in $5d$ systems the extended orbitals result in enhanced collective behavior within the lattice compared to, for example, that which occurs in $3d$ transition metal oxides. Indeed, this was shown in NaOsO₃ with the observation of a record large spin-phonon shift at the MIT due to the extended Os orbitals [15].

The measurement of a large spin gap indicates that SOC is required in a complete description of NaOsO₃. The magnitude of SOC scales with the atomic number, therefore, in 5d³ osmates it is comparable to 5d⁵ iridates. However, when describing the properties of NaOsO₃, the role of SOC has only been required to be included as a perturbation [6,7,11–15]. Conversely, for 5d⁵ iridates, SOC is necessary to describe both magnetism and the insulating state. This has created an apparent dichotomy between the effect of SOC, particularly when considering the divergent electronic ground states indicated from the RIXS spectra between 5d³ and 5d⁵. A first approximation is that the altered electronic occupancy causes an increased Hund's coupling in 5d³ systems, favoring a quenching of orbital momentum. However, the broad scattering observed for E_B in Fig. 1 indicates an underlying splitting of the t_{2g} orbitals, either through structural distortions or SOC or a combination of both. One consequence of an increased role of SOC in NaOsO₃ was considered theoretically to reduce the effective U and place the system closer to the itinerant limit description of magnetism [23]. However, the agreement of the minimal model Hamiltonian, based on localized spins, to the RIXS spectra would suggest that the behavior of NaOsO₃ appreciably departs from being fully itinerant. Indeed, this would be expected even within the mean-field Hartree-Fock description used by Slater to describe a magnetic MIT since, at the transition, local moments are necessarily formed [24]. While in a pure Slater description this would be treated by self-consistent single electron theory, at least to a good approximation the behavior can be described by a Heisenberg model and places NaOsO₃ on the boundary between local-moment and itinerant magnetism.

The strongly dispersing excitation in NaOsO₃ contrasts with the dispersionless excitation of Cd₂Os₂O₇ observed previously with RIXS [18]. The use of an Ising-like description to describe Cd₂Os₂O₇ and a Heisenberg model to capture the behavior for NaOsO₃ may indicate distinct magnetic interactions in these two closely related materials. While the behavior appears to diverge, indicating the potential for varied and exotic phenomena in related 5d³ oxides, for both osmates the magnetic excitation spectra reveal an appreciable influence of SOC.

The 5d orbital and collective magnetic excitations in NaOsO₃ have been probed with RIXS. Well-defined spin waves were observed and described within linear spin-wave theory using a minimal model Hamiltonian that captured the essential features. Nearest- and next-nearest-neighbor Heisenberg exchange interactions of $J_1 = J_2 = 13.9$ meV were found to describe the dispersion, indicating strong three-dimensional magnetic interactions. The presence of significant anisotropy in the system was observed with the measurement of a large spin gap of 58 meV. This is a direct consequence of intrinsically strong SOC in this 5d compound, however, the role of SOC on the ground state departs from 5d⁵ iridates. In terms of the mechanism of the MIT, the results support a three-dimensional magnetically driven route, consistent with the general scenario proposed by Slater. The Hamiltonian presented here provides the magnetic interaction energy scales and their pathways required to describe the MIT. Moreover, the presence of SOC and the influence this has within a system with extended orbitals and strong hybridization has to be considered as playing an important role when considering the collective interactions and the MIT.

A.D.C. thanks A. E. Taylor for useful discussions. We thank C. Henriquet and R. Verbeni at the ESRF for the design and manufacture of the high-temperature stage. Preliminary measurements were performed at 9-ID-B and 30-ID (MERIX), APS, which is a U.S. Department of Energy (DOE) Office of Science User Facility operated for the DOE Office of Science by Argonne National Laboratory under Contract No. DE-AC02-06CH11357. This research used resources at the High Flux Isotope Reactor and Spallation Neutron Source, a DOE Office of Science User Facility operated by the Oak Ridge National Laboratory. This work in London was supported by the UK Engineering and Physical Sciences Research Council (EPSRC). J.G.V. would like to thank UCL and EPFL for financial support via a UCL Impact Studentship. X.L. acknowledges financial support from MOST (No. 2015CB921302) and CAS (No. XDB07020200) of China. Work done at Brookhaven National Laboratory was supported by US DOE, Division of Materials Science, under Contract No. DE-SC00112704. K.Y. thanks financial support from JSPS KAKENHI (15K14133 and 16H04501).

-
- [1] M. Imada, A. Fujimori, and Y. Tokura, *Rev. Mod. Phys.* **70**, 1039 (1998).
- [2] W. Witczak-Krempa, G. Chen, Y. B. Kim, and L. Balents, *Annu. Rev. Condens. Matter Phys.* **5**, 57 (2014).
- [3] B. J. Kim, H. Ohsumi, T. Komesu, S. Sakai, T. Morita, H. Takagi, and T. Arima, *Science* **323**, 1329 (2009).
- [4] D. Mandrus, J. R. Thompson, R. Gaal, L. Forro, J. C. Bryan, B. C. Chakoumakos, L. M. Woods, B. C. Sales, R. S. Fishman, and V. Keppens, *Phys. Rev. B* **63**, 195104 (2001).
- [5] J. Yamaura, K. Ohgushi, H. Ohsumi, T. Hasegawa, I. Yamauchi, K. Sugimoto, S. Takeshita, A. Tokuda, M. Takata, M. Udagawa, M. Takigawa, H. Harima, T. Arima, and Z. Hiroi, *Phys. Rev. Lett.* **108**, 247205 (2012).
- [6] Y. G. Shi, Y. F. Guo, S. Yu, M. Arai, A. A. Belik, A. Sato, K. Yamaura, E. Takayama-Muromachi, H. F. Tian, H. X. Yang, J. Q. Li, T. Varga, J. F. Mitchell, and S. Okamoto, *Phys. Rev. B* **80**, 161104 (2009).
- [7] S. Calder, V. O. Garlea, D. F. McMorrow, M. D. Lumsden, M. B. Stone, J. C. Lang, J.-W. Kim, J. A. Schlueter, Y. G. Shi, K. Yamaura, Y. S. Sun, Y. Tsujimoto, and A. D. Christianson, *Phys. Rev. Lett.* **108**, 257209 (2012).
- [8] P. W. Anderson, *Phys. Rev.* **109**, 1492 (1958).
- [9] R. E. Peierls, *Quantum Theory of Solids* (Oxford University Press, New York, 1955).
- [10] J. C. Slater, *Phys. Rev.* **82**, 538 (1951).
- [11] Y. Du, X. Wan, L. Sheng, J. Dong, and S. Y. Savrasov, *Phys. Rev. B* **85**, 174424 (2012).

- [12] M.-C. Jung, Y.-J. Song, K.-W. Lee, and W. E. Pickett, *Phys. Rev. B* **87**, 115119 (2013).
- [13] I. L. Vecchio, A. Perucchi, P. Di Pietro, O. Limaj, U. Schade, Y. Sun, M. Arai, K. Yamaura, and S. Lupi, *Sci. Rep.* **3**, 2990 (2013).
- [14] S. Middey, S. Debnath, P. Mahadevan, and D. D. Sarma, *Phys. Rev. B* **89**, 134416 (2014).
- [15] S. Calder, J. H. Lee, M. B. Stone, M. D. Lumsden, J. C. Lang, M. Feyngenson, Z. Zhao, J.-Q. Yan, Y. G. Shi, Y. S. Sun, Y. Tsujimoto, K. Yamaura, and A. D. Christianson, *Nat. Commun.* **6**, 8916 (2015).
- [16] E. Kermarrec, C. A. Marjerrison, C. M. Thompson, D. D. Maharaj, K. Levin, S. Kroecker, G. E. Granroth, R. Flacau, Z. Yamani, J. E. Greedan, and B. D. Gaulin, *Phys. Rev. B* **91**, 075133 (2015).
- [17] A. E. Taylor, R. Morrow, R. S. Fishman, S. Calder, A. I. Kolesnikov, M. D. Lumsden, P. M. Woodward, and A. D. Christianson, *Phys. Rev. B* **93**, 220408(R) (2016).
- [18] S. Calder, J. G. Vale, N. A. Bogdanov, X. Liu, C. Donnerer, M. H. Upton, D. Casa, A. H. Said, M. D. Lumsden, Z. Zhao, J. Q. Yan, D. Mandrus, S. Nishimoto, J. van den Brink, J. P. Hill, D. F. McMorrow, and A. D. Christianson, *Nat. Commun.* **7**, 11651 (2016).
- [19] J. Kim, D. Casa, M. H. Upton, T. Gog, Y.-J. Kim, J. F. Mitchell, M. van Veenendaal, M. Daghofer, J. van den Brink, G. Khaliullin, and B. J. Kim, *Phys. Rev. Lett.* **108**, 177003 (2012).
- [20] M. Moretti Sala, S. Boseggia, D. F. McMorrow, and G. Monaco, *Phys. Rev. Lett.* **112**, 026403 (2014).
- [21] Diagonalizing the Hamiltonian in Eq. (1) within a LSW approximation gives the spin-wave energy ω , $\omega = S\sqrt{D - X - Y}$, where $D = 36\Delta^2 + 48\Delta J_1 + 24\Delta J_2 + 12J_1^2 + 2J_2^2 + 16J_1J_2$, $X = 4J_1^2 \cos 2\pi h + 2J_2^2 \cos 2\pi h + 4J_1^2 \cos 2\pi l$, and $Y = 2J_1^2 \cos [2\pi(h - l)] + 2J_1^2 \cos [2\pi(h + l)] + 16J_1J_2 \cos \pi h \cos \pi k \cos \pi l$. In a similar fashion, the intensity can be expressed by $S(q, \omega) = S[\frac{D-(X-Y)}{D-(X+Y)}] \delta(\omega, \omega_q)$.
- [22] S. Toth and B. Lake, *J. Phys.: Condens. Matter* **27**, 166002 (2015).
- [23] B. Kim, P. Liu, Z. Ergonen, A. Toschi, S. Khmelevskyi, and C. Franchini, *Phys. Rev. B* **94**, 241113 (2016).
- [24] F. Gebhard, *The Mott Metal-Insulator Transition* (Springer, Berlin, 1997).